

# Mechanical properties of BaTiO<sub>3</sub> open-porosity foams

Laurel Wucherer<sup>a,\*</sup>, Juan C. Nino<sup>a</sup>, Ghatu Subhash<sup>b</sup>

<sup>a</sup> Department of Materials Science & Engineering, University of Florida, Gainesville, FL 32611, USA

<sup>b</sup> Department of Mechanical & Aerospace Engineering, University of Florida, Gainesville, FL 32611, USA

Received 11 November 2008; accepted 22 December 2008

Available online 1 February 2009

## Abstract

Barium titanate (BaTiO<sub>3</sub>) foams synthesized via direct foaming method using silicon-free, rigid polyurethane systems (PU), commercially purchased and lab developed, are being engineered for piezocomposites in sonar applications. The mechanical properties of these foams were measured using confined compression testing to evaluate the suitability of these foams for the intended application. Compressive modulus and collapse strain determined from the experimental data increased with increasing density. Additionally, the foams fabricated using the lab developed PU (LPU) showed a higher mechanical strength due to a higher average density than the foams developed using commercial PU (CPU) system. The data was then fit with a phenomenological model to verify the values of the compressive properties extracted from the experimental data and also to extract additional properties such as tensile strength. Based on these findings, it is proposed that these foams can be successfully incorporated into piezocomposites by infiltrating the foams with polymer.  
© 2009 Elsevier Ltd. All rights reserved.

**Keywords:** Porosity; Mechanical properties; BaTiO<sub>3</sub>; Sensors

## 1. Introduction

Ceramic foams offer a favorable and unique combination of mechanical and functional properties. In a previous study,<sup>1</sup> the authors have synthesized barium titanate (BaTiO<sub>3</sub>) foams using the direct foaming method. It was found that the microstructure of the ceramic foam could be controlled by proper selection of PU system, ceramic composition, sintering time and sintering temperature. An open-structure foam with dense, rounded struts composed of a few larger grains (20–45 μm) was produced at a high sintering temperature (1400 °C) and an intermediate sintering time (8 h).<sup>1</sup> The optimal ceramic content was determined to be 30 vol% and the rest was PU. It was found that the variability in density for these foams was not significant.

In this study, two different rigid, Si-free polyurethane systems, one commercially purchased (CPU) and the other laboratory developed (LPU) were used. Although these foams are primarily intended for sensing and actuation, their ability to withstand stress and deformation is also important for handling purposes as well as to ensure mechanical integrity at high

stress levels during service. Among many desirable properties, the compressive behavior is of prime importance. In literature, mechanical properties of 1–3<sup>2</sup> and 0–3<sup>3</sup> composites have been reported but very little has been reported on mechanical properties of 3–3 composites. A typical 1–3 composite consists of rods in a matrix in which ceramic rods are held parallel by a passive polymer matrix.<sup>2</sup> For underwater sensor application it is important that the acoustic impedance of the composite be similar to that of water (1.569 MRayls).<sup>3</sup> While recent breakthroughs have been made with 1–3 composites in achieving this low acoustic impedance,<sup>4</sup> 3–3 composites offer a good balance between a polymer with low acoustic impedance, and a piezoelectric ceramic with high mechanical strength and piezoelectric properties. However, for good mechanical stability, the strengths of both the ceramic foam and the polymer must be enhanced.

For polymeric foams, Liu and Subhash<sup>5</sup> proposed a phenomenological model that can capture the entire compressive stress–strain response. In general, the stress–strain response of porous materials subjected to compressive loads has three distinct zones; (i) an elastic region, (ii) a plateau region and (iii) a densification region. The plateau region is associated with the collapse of the porous, cellular structure which gives the foam its energy absorption ability. For the piezo-sensor application, the primary focus is on the elastic region due to the requirement

\* Corresponding author. Tel.: +1 407 421 3874; fax: +1 352 846 3355.  
E-mail address: [laureli@ufl.edu](mailto:laureli@ufl.edu) (L. Wucherer).

of reversible deformation. Therefore, only the early portion of stress–strain response that includes elastic and partial collapse strains are used for modelling and property determination. In this work it is shown that the mechanical properties of the ceramic foam fabricated by the above mentioned method are comparable to other ceramic foams<sup>6,7</sup> and thus, possibly suitable for sensor applications.

## 2. Experimental procedure

BaTiO<sub>3</sub> foam samples were synthesized using two rigid, Si-free polyurethane systems: (i) commercially purchased (CPU) from Smooth-On (Easton, PA) and (ii) laboratory developed system (LPU) by Traversa et al. at the University of Rome – Tor Vergata.<sup>8</sup> Following the previously reported processing steps, 28–32 vol% BaTiO<sub>3</sub> was foamed and sintered for mechanical testing.<sup>1</sup> For brevity only a short discussion is presented here.

A mixture of 28–32 vol% ceramic powder and 70 vol% PU are used as the precursor materials. The ceramic powder is weighed so that 30 vol% is ceramic and 70 vol% of the mixture is PU. The materials are combined and stirred until the mixture is highly viscous due to the foaming process. The mixture is then set aside to complete foaming. The foam is cured for 24 h at room temperature before being sintered at 1400 °C for 8 h to produce a purely ceramic foam.

BaTiO<sub>3</sub> foams produced from the above two systems were cut into 12.7 mm diameter specimens using a tape cast hole punch. Five specimens were made for each system. The density of foam was systematically varied by varying the initial ceramic content from 28 to 32 vol%. It was earlier found that the variability in density from one foam specimen to another was small (0.08%) when the initial ceramic content was kept constant; therefore, only one sample was made for each density and the difference in mechanical properties of foams produced from the two PU systems was determined. The apparent density and open porosity of each specimen was measured using helium pycnometry. These values are provided in Table 1. It is shown that the LPU foams were denser due to a smaller expansion during the foaming process but they also had a larger change in density for a small change in ceramic content, compared to CPU foams. Uniaxial compression experiments were performed at room temperature using a MTS universal testing machine (UTM). Each specimen was marked with a grid of horizontal lines to track the uniformity of deformation during the test.

Table 1  
Porosity and density values for the BaTiO<sub>3</sub> foam specimens.

Ceramic content (vol%)	Porosity (%)		Density (g/cm <sup>3</sup> )	
	CPU	LPU	CPU	LPU
32	87.0	80.0	0.78	1.20
31	88.0	84.7	0.72	0.92
30	91.0	85.3	0.54	0.88
29	93.0	86.3	0.42	0.82
28	93.7	92.8	0.38	0.43
Average	90.6	85.8	0.57	0.82
S.D.	2.95	4.6	0.18	0.28

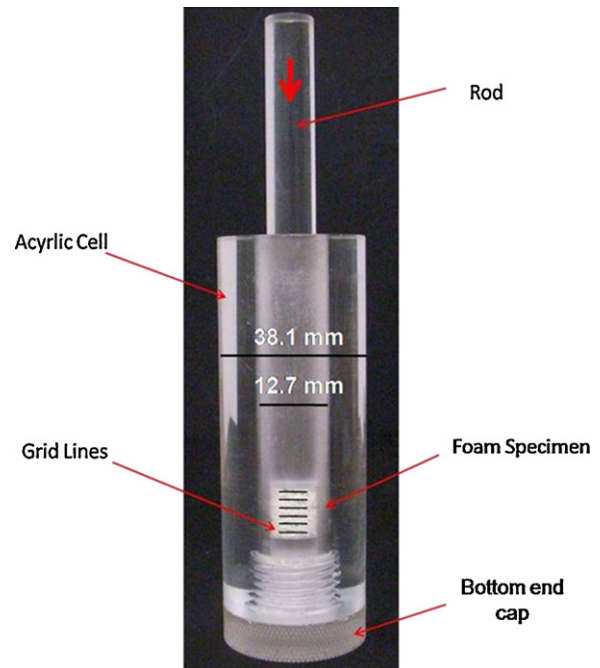


Fig. 1. Confinement cell and foam sample used for confined compression testing.

In the authors' previous work,<sup>1</sup> it was noted that when these foam specimens were loaded without any lateral confinement, they deformed unevenly along the length of the specimen.<sup>5</sup> This behavior was due to premature collapse of large porous cells that lie along the outer surface. The collapse then led to instabilities resulting in buckling of the entire specimen. Such buckling modes are typically observed in commercial brittle polymeric foams.<sup>9</sup> To avoid this mode of failure it was decided to test the specimens in a transparent confinement cell as shown in Fig. 1. This confinement was previously proposed and used by Walter et al.<sup>9</sup> The transparent, cylindrical cell was made of acrylic and consisted of a sliding cylindrical rod and an end cap that can be screwed to the bottom of the cylinder. The ceramic foam specimen is placed inside the cell and pushed to the bottom by a cylindrical rod. The entire assembly is placed in the MTS machine and loaded at a displacement rate of 1.27 mm/min resulting in a strain rate of 0.001 s<sup>-1</sup>.

## 3. Results and discussion

### 3.1. Foam synthesis

Fig. 2 shows the microstructure of the BaTiO<sub>3</sub> foams synthesized via direct foaming method using both PU systems. The microstructural features of these foams reveal an open cell structure with dense, rounded struts consisting of a few intermediate sized grains. This microstructure is different from the previously fabricated foams by Colombo et al.<sup>6</sup> and Costa Oliveira et al.<sup>7</sup> which produced struts that were either hollow, had sharp wall edges, or consisted of many small (few μm) grains. This microstructure is similar to the one reported previously by the authors.<sup>1</sup> Both ceramic foams were resilient during handling

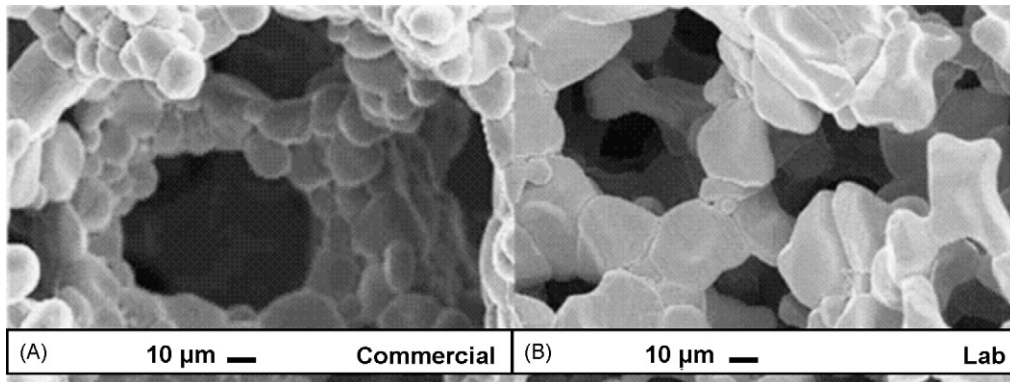


Fig. 2. SEM image of 30 vol% barium titanate foam synthesized using (A) CPU and (B) LPU system.

and revealed homogenous microstructures as determined from SEM and image analysis. The foam produced by CPU system had larger and more interconnected cell windows ( $98\ \mu\text{m}$ ) and struts consisting of approximately  $20\ \mu\text{m}$  grains, while the foam produced by LPU system had smaller cell windows ( $67\ \mu\text{m}$ ) and struts with large  $45\ \mu\text{m}$  grains.

### 3.2. Confined compression testing

The compressive engineering stress–strain responses of the different ceramic foams are presented in Figs. 3 and 4. Because the focus of the work was on the elastic region of the response, the samples were strained just beyond yield point. Similar to any cellular material behavior, the ceramic foams exhibited an initial elastic response followed by a cell collapse process which results in the plateau region. The stress–strain response was strongly dependent on initial foam density. Both the initial slope and the collapse stress increased with density for both PUs. The slopes were highly nonlinear and therefore the stiffness was incrementally calculated and averaged over the elastic range.

Mechanical properties extracted from the above plots are summarized in Table 2. The compression modulus ( $E_C$ ) and collapse stress ( $\sigma_C$ ) values of the CPU and LPU foams determined from the above stress–strain responses are plotted with

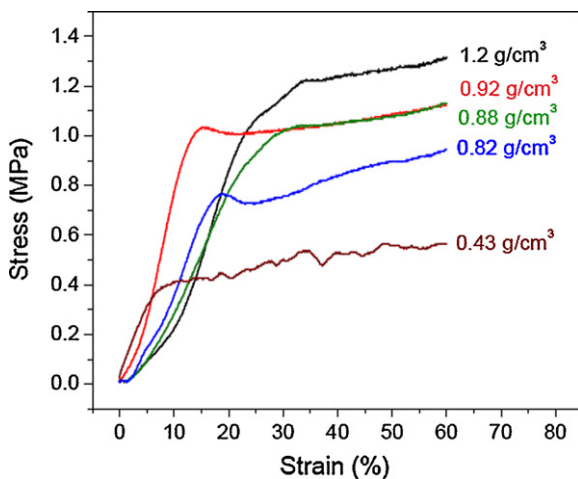


Fig. 3. Stress–strain response of  $\text{BaTiO}_3$  foam produced from LPU system.

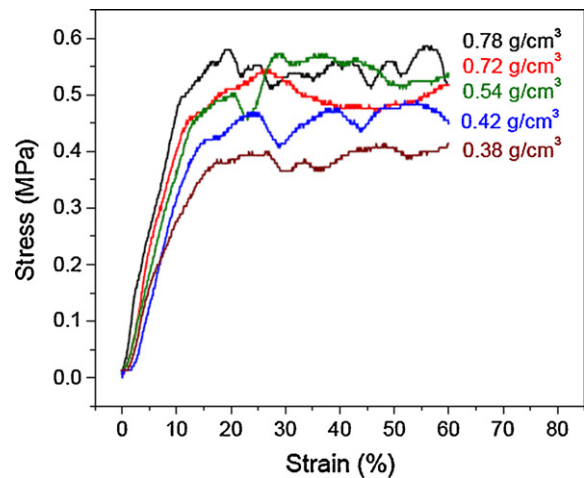


Fig. 4. Stress–strain response of  $\text{BaTiO}_3$  foam produced from CPU system.

respect to density in Fig. 5. Although both material properties increase with increasing density for both foams, a significantly higher rate of increase is observed in foam produced by LPU. As expected, the LPU foams had on average a higher modulus and collapse stress due to the higher density. A better comparison of mechanical properties of foams can be seen in Fig. 6 where the stress–strain curves at two different foam densities are compared. Clearly, for approximately similar foam density, a greater collapse stress is observed in LPU foam than in CPU foam.

As mentioned earlier, the foams were marked with equally spaced grid lines to track the uniformity of deformation and the collapse process. Figs. 7 and 8 illustrate the deformation

Table 2  
Comparison of mechanical properties.

Ceramic content (vol%)	$E_C$ (MPa)		$\sigma_C$ (MPa)	
	CPU	LPU	CPU	LPU
32	4.99	9.69	0.93	1.25
31	4.71	7.77	0.60	1.07
30	4.64	6.69	0.54	1.06
29	4.06	6.08	0.51	1.02
28	3.67	4.39	0.39	0.78
Average	4.41	6.92	0.59	0.91
S.D.	0.53	1.97	0.21	0.32

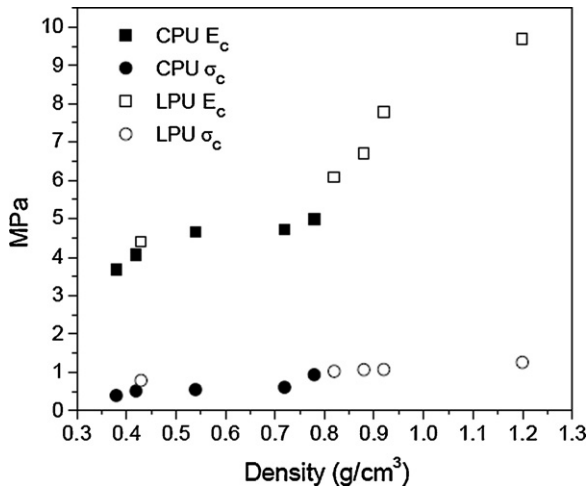


Fig. 5. Mechanical properties of barium titanate foam as a function of density.

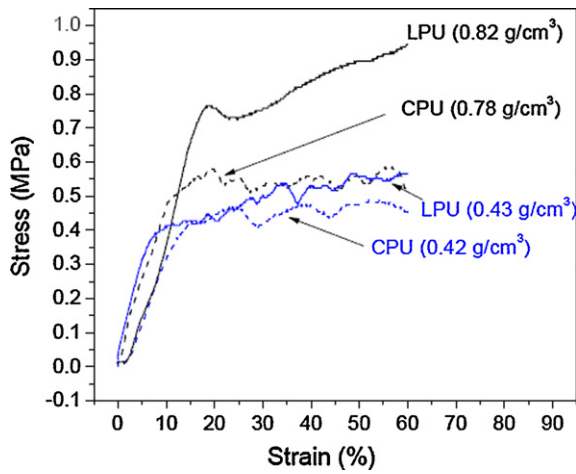


Fig. 6. Stress–strain curves comparing density and PU.

behavior of the foams at various strain levels. The grid lines in Figs. 7 and 8 are digitally enhanced to distinguish the lines since some are diffused due to the porous surface. Note that all these lines remain relatively straight throughout the deformation process. In foams with relatively large pore sizes, these lines become nonlinear and the spacing between the lines becomes uneven very early on in the deformation process due to the collapse of isolated large cells.<sup>10,11</sup> Such features were not observed in the BaTiO<sub>3</sub> foams because the pore size is relatively small and uniform and therefore, the spacing between any two lines remains relatively constant along the length. However, the spacing between the lines decreases with strain as the cells start to collapse uniformly. There is one noticeable difference between the deformation behavior of LPU and CPU foams. In the LPU foams, the deformation is not uniform along the length of the specimen. Note that the line spacing on the top decreases more rapidly than the spacing at the bottom. This indicates that the deformation in this foam is more progressive rather than uniform throughout the specimen.

The deformation progresses from the top of the specimen to the bottom of the specimen with increasing load, i.e., there is a sequential collapse of cells with load. On the other hand, the deformation of foams made from CPU is comparatively more uniform, as indicated by the continued reduction in the spacing of most of the lines with increasing strain (Fig. 8). The BaTiO<sub>3</sub> foam struts have an average thickness of 60 μm and consist of a few intermediate size grains (~20 μm), determined using image analysis of SEM images. According to Li et al.,<sup>12</sup> the thickness of the cell wall or strut is directly correlated with the strength of the foam; therefore, all others being equal, it is expected that thicker struts will lead to a stronger BaTiO<sub>3</sub> foam. Most piezo-sensors in the market today are made of bulk electroceramic materials such as PZT<sup>13</sup> and have higher mechanical strength compared to the foams shown in Table 3. In future work, the intent is to infiltrate these foams with a polymer to enhance mechanical properties and possibly piezoelectric properties depending

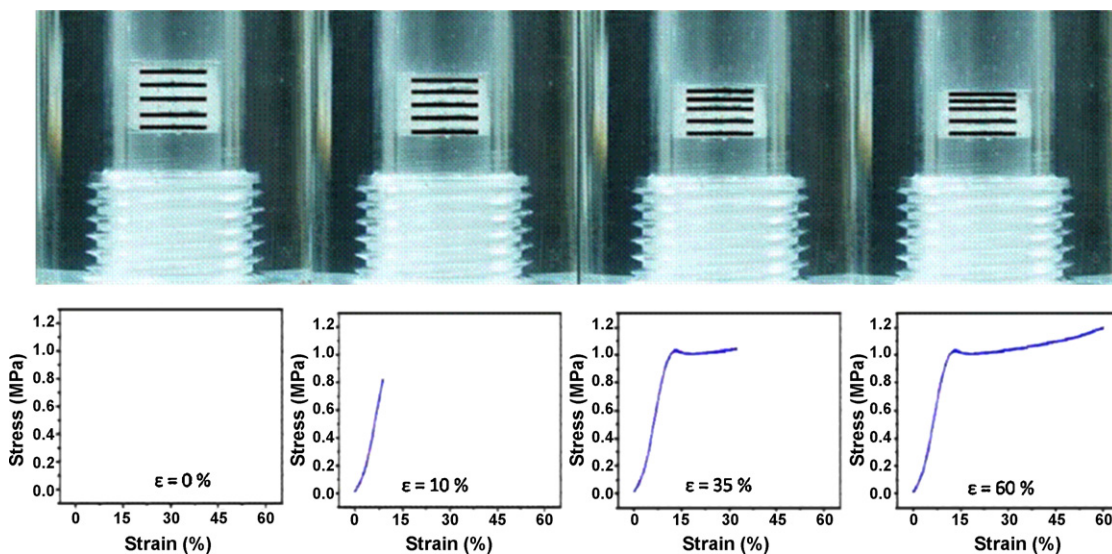


Fig. 7. Compression of LPU foam with respective stress–strain curves.

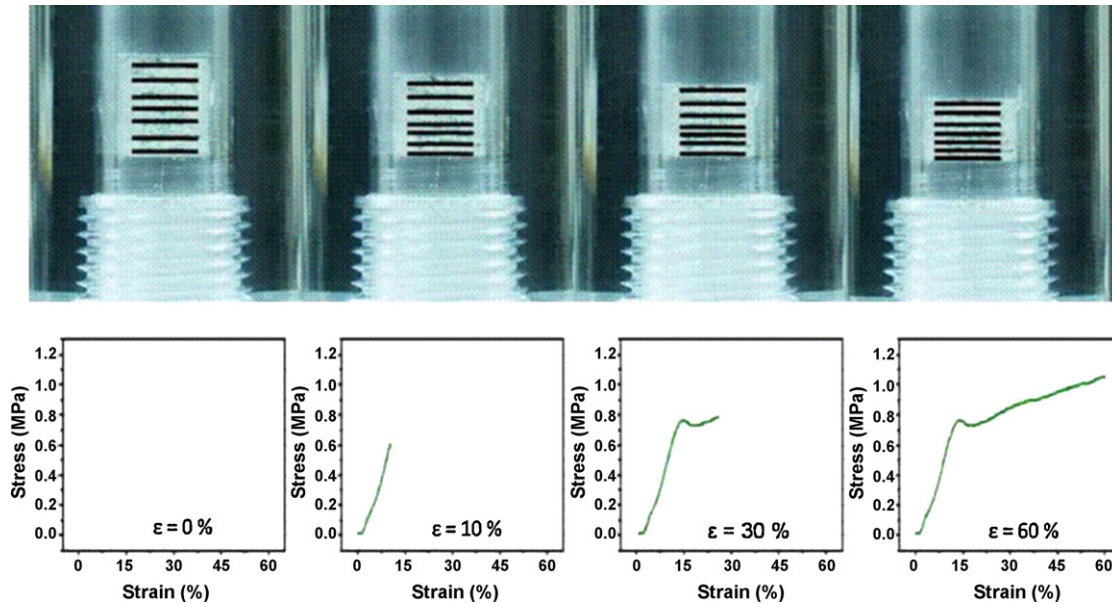


Fig. 8. Compression of CPU foam with respective stress–strain curves.

on the polymer selected. The required mechanical strength of a piezoelectric material for sensor applications is yet to be reported. While the mechanical properties of the BaTiO<sub>3</sub> foam skeleton are not yet comparable to other composites, such as the 1–3 ceramic rod composites by Smith<sup>2</sup> ( $E \sim 31$  GPa for 25% PZT rod composite), the ceramic foam could still be acceptable for sensor applications and will be determined once a prototype piezocomposite sensor has been fabricated. It must also be noted that the mechanical properties of the foams presented here are not yet optimized. While the stress required may vary with application, suggestions for increasing the mechanical strength of the foam include increasing the ceramic content to 40 vol% or modifying the grain size by altering the sintering temperature. In addition, infiltration with polymer is expected to increase the compliance of the compressive behavior and enhance the relaxation behavior of the composite, while lowering the acoustic impedance of the overall sensor. For such applications it is important to maintain a balance between mechanical properties and electrical properties of the piezocomposite. Therefore the current method of producing foams and the resulting microstructure are expected to produce an acceptable balance between the two properties, thus making it suitable for sensor application.

### 3.3. Stress–strain phenomenological model

The stress–strain behavior of the foams presented here reveals an elastic response followed by an inelastic response that con-

sists of the cell collapse in the foam. If the compressive load was continued, the foams would have exhibited a densification regime which is typical of any cellular material. This complex behavior was captured using the following phenomenological model by Liu and Subhash<sup>5</sup>

$$\sigma = A \frac{e^{\alpha\epsilon} - 1}{B + e^{\beta\epsilon}} + ke^C(e^{\gamma\epsilon} - 1) \quad (1)$$

where  $\sigma$  is uniaxial stress,  $\epsilon$  the uniaxial strain, and  $A$ ,  $B$ ,  $C$ ,  $\alpha$ ,  $\beta$  and  $\gamma$  are parameters that describe various features of the stress–strain response. The value  $k$  equals 1 with units of stress. In Eq. (1), the parameter  $A$  represents the yield stress (or collapse stress) and parameter  $B$  represents the ratio of ultimate tensile strength to collapse stress.<sup>9</sup> Parameters  $\alpha$  and  $\beta$  describe the plateau region of the stress–strain response. For  $\alpha > \beta$  a hardening-like behavior is observed.  $\alpha = \beta$  represents the perfectly-plastic response and  $\alpha < \beta$  represents a softening-like behavior.

The first term in the model capture the elastic response and the cell collapse process whereas the second term captures the densification response. However, the interest is only in the early part of the response consisting of the elastic and cell collapse regimes, as shown in Figs. 9 and 10. Only the first term in the above phenomenological model was used to fit these stress–strain curves.

Recently Walter et al.<sup>9</sup> extended the above model to both compression and tensile regimes and were able to determine several other parameters through extensive experimentation on five different density foams. The advantage of such a model is that one can determine the response of foam at intermediate densities that were not originally available. The model can also calculate tensile strength of the foam as will be described below.

By fitting the experimental data with the first term in Eq. (1), we can obtain the model parameters described above ( $\alpha$ ,  $A$ , and  $B$ ). The relationship between the model parameters and

Table 3  
Properties and of various ceramic foams and commercial PZT.

Parameter	BaTiO <sub>3</sub> foam LPU	BaTiO <sub>3</sub> foam CPU	Bulk PZT <sup>12</sup>
$\rho$ (g/cm <sup>3</sup> )	0.43	0.42	7.6
$E$ (MPa)	4.39	3.78	66,000
$\sigma_C$ (MPa)	0.78	0.47	>517

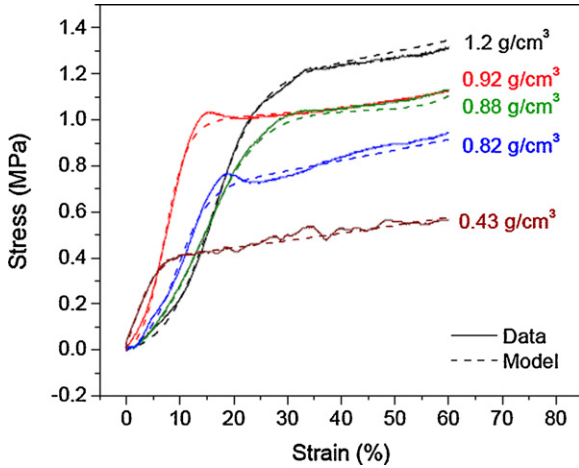


Fig. 9. Measured data and model fit for BaTiO<sub>3</sub> foam produced by LPU.

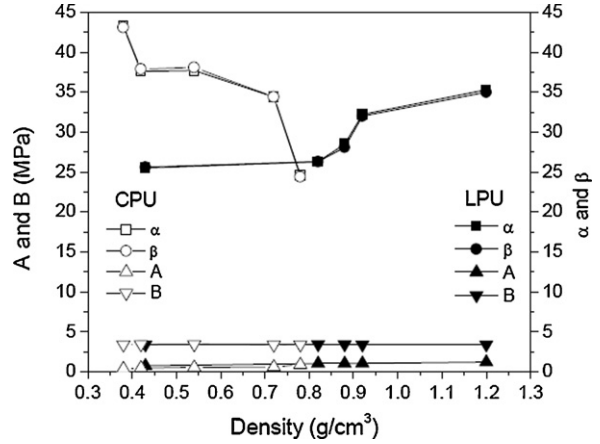


Fig. 11. Model parameters as a function of density.

foam mechanical properties were determined by Walter et al.<sup>9</sup> as follows:

$$A \approx \sigma_C \tag{2}$$

$$B \approx \frac{\sigma_C}{\sigma_{ult}} \tag{3}$$

$$E = \frac{A\alpha}{1+B} \tag{4}$$

Here  $\sigma_{ult}$  is the ultimate tensile strength and  $\sigma_C$  is the compressive collapse strength.

Figs. 9 and 10 show the comparison between the experimental data and the model fit for the LPU and the CPU-BaTiO<sub>3</sub> foams with approximately similar densities. As shown, the model accurately captures both the elastic and plateau regions, therefore with the parameters determined from the model, the compressive modulus and collapse stress can be accurately calculated using the equations listed above.

Fig. 11 illustrates the trends in model parameters as a function of density. The difference in trends for  $\alpha$  and  $\beta$  between CPU and LPU is purely mathematical and due to the fact that the collapse stresses for CPU are under 1 MPa and the collapse stresses

for LPU are above 1 MPa. For the ceramic foams,  $A$  increases slightly with density and  $B$  remains relatively constant, indicating that for all of the densities the collapse stress is  $\sim 3.4$  times larger than the ultimate tensile strength of the foams.

The values of the modulus and collapse stress obtained from the model are comparable to the values determined previously from the measured data as seen in Fig. 12. Clearly, the model captures the experimental data well. Therefore, the model can now be extended to other density foam within the range of densities tested here because the trends in the model parameters, Fig. 11, are now known. We can also determine the ultimate tensile strength of the foams using Eq. (3). Note that, unlike the compressive response where large strains are noted, brittle foams exhibit small strain in tension before failure Fig. 13 presents the expected ultimate tensile stresses ( $\sigma_{ult}$ ) of the ceramic foams as determined using Eq. (3). As expected, the tensile strength of the BaTiO<sub>3</sub> foams is significantly less than the compressive strength due to the inherent brittle behavior of ceramics. The ultimate tensile strength increases with density. Interestingly, it is noted that the tensile strength of the LPU foams increase linearly whereas tensile strength of the CPU foams increase nonlinearly.

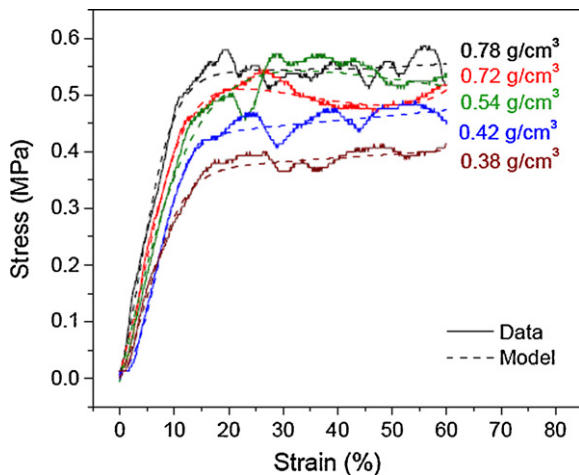


Fig. 10. Measured data and model fit for BaTiO<sub>3</sub> foam produced by LPU.

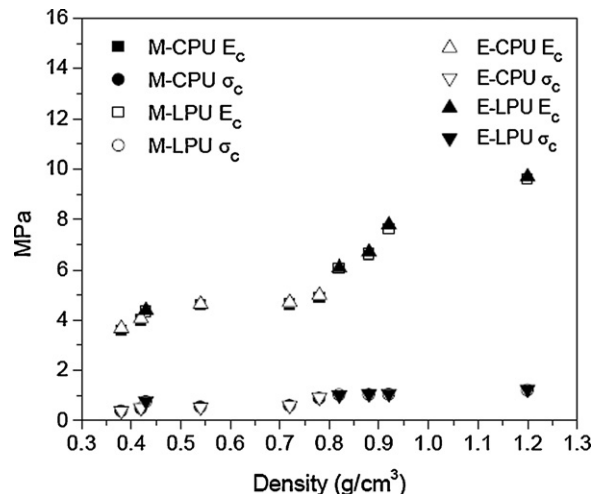


Fig. 12. Comparison of mechanical properties determined from the (M-) fitted data and (E-) experimental data as a function of density.

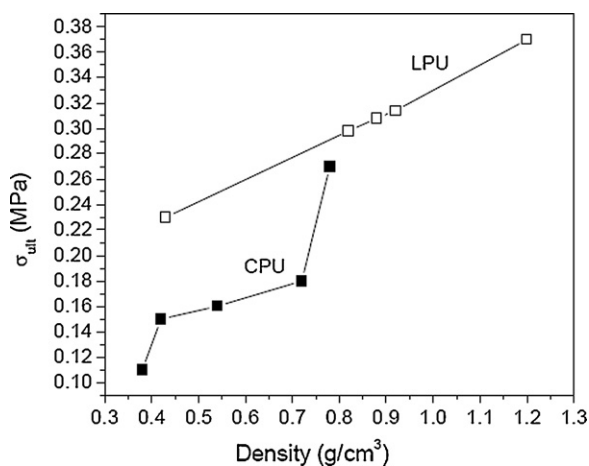


Fig. 13. Model estimated ultimate tensile strength of BaTiO<sub>3</sub> foams as a function of density.

More in-depth experimentation and model analysis is required to further validate these values in this class of ceramics.

The properties determined here provide a starting point for optimization of the foams in future studies were the ceramic foams will be infiltrated with polymeric materials for enhanced piezoelectric effect.

#### 4. Conclusion

The mechanical properties of BaTiO<sub>3</sub> foams synthesized via direct foaming method using a commercial and a laboratory developed rigid, Si-free polyurethane systems were determined using confined compression testing. There was an increase in modulus and collapse strength with increasing density in both foams. The LPU foams were denser compared to the CPU foams (0.82 g/cm<sup>3</sup> vs. 0.51 g/cm<sup>3</sup>), and hence had a higher modulus (6.92 MPa) and collapse strength (0.91 MPa) than the CPU foam (4.16 and 0.47 MPa, respectively). The mechanical properties of LPU foam are more strongly dependent on density than CPU foams.

The phenomenological model proposed by Liu and Subhash<sup>5</sup> captured the elastic and plateau regions of the compressive behavior reasonably well. The model parameters determined

also compare well with the experimentally determined properties.

Based on this work, it is suggested that these ceramic foams have good mechanical properties and the potential for electromechanical applications such as piezo-sensors where they can be infiltrated with a polymer to create a piezocomposite with enhanced piezoelectric and mechanical properties.

#### References

1. Wucherer, L., Nino, J. C., Basoli, F. and Traversa, E., Synthesis and characterization of BaTiO<sub>3</sub>-based foams with controlled microstructure. *Int. J. Appl. Ceram.*, in press.
2. Smith, W. A., The role of piezocomposites in ultrasonic transducers. In *Ultra. Symp., Proc. IEEE*, vol. 2, 1989, pp. 755–766.
3. Cross, L. E., Ferroelectric ceramics: tailoring properties for specific applications. *Ferroelectric Ceramics: Tutorial Reviews, Theory, Processing, and Applications*. Birkhauser, Basel, 1993.
4. Smith, W. A. and Auld, B. A., Modeling 1–3 composite piezoelectrics: thickness-mode oscillations. *Ultra Ferro. Freq. Control IEEE*, 1991, **38**(1), 40–47.
5. Liu, Q. and Subhash, G., A phenomenological constitutive model for foams under large deformations. *Polym. Eng. Sci.*, 2004, **44**(3), 463–473.
6. Colombo, P., Hellmann, J. R. and Shelleman, D. L., Mechanical properties of silicon oxycarbide ceramic foams. *Comp. Sci. Technol.*, 2001, **63**(16), 2245–2251.
7. Costa Oliveira, F. A., Dias, S., Fatima Vaz, M. and Cruz Fernandes, J., Behavior of open-cell cordierite foams under compression. *J. Eur. Ceram. Soc.*, 2006, **26**(1–2), 179–186.
8. Rainer, A., Basoli, F., Licoccia, S. and Traversa, E., Foaming of filled polyurethanes for fabrication of porous anode supports for IT-SOFC. *J. Am. Ceram. Soc.*, 2006, **6**(89), 1795–1800.
9. Walter, T. R., Richards, A. W. and Subhash, G., A unified phenomenological model for compression and tension response of polymer foams. *ASME J. Eng. Mater. Technol.*, 2008, **131**(1), Art. No. 011009.
10. Liu, Q., Subhash, G. and Gao, X.-L., A parametric study on crushability of open-cell structural polymeric foams. *J. Porous Mater.*, 2005, **2**(3), 233–248.
11. Subhash, G., Liu, Q. and Gao, X.-L., Quasistatic and high strain rate uniaxial compressive response of polymeric structural foams. *Int. J. Impact Eng.*, 2006, **7**(32), 1113–1126.
12. Li, K., Gao, X. L. and Subhash, G., Effects of cell shape and cell wall thickness variations on the elastic properties of two-dimensional cellular solids. *Int. J. Solids Struct.*, 2005, **42**(5–6), 1777–1795.
13. Morgan Technical Ceramics, Piezoelectric Material Technical Bulletin, Bedford, OH, <http://www.morganelectroceramics.com/piezomaterials/pzmat5.html>.